



Original scientific paper

## Development of CNT reinforced Al<sub>2</sub>O<sub>3</sub>-TiO<sub>2</sub> coatings for boiler tubes to improve hot corrosion resistance

Rakesh Goyal<sup>1,✉</sup> and Khushdeep Goyal<sup>2</sup>

<sup>1</sup>Chitkara University Institute of Engineering & Technology, Chitkara University, Punjab, India

<sup>2</sup>Mechanical Engineering Department, Punjabi University, Patiala, India

Corresponding author: ✉ [rakesh.goyal@chitkara.edu.in](mailto:rakesh.goyal@chitkara.edu.in)

Received: February 9, 2022; Accepted: July 25, 2022; Published: August 31, 2022

### Abstract

This study examines the hot corrosion behaviour of plasma-coated T12 steel for 10 cycles of 100 h each in an industrial boiler. The coating contains CNT (carbon nanotubes) reinforced alumina-titania powders. The substrates were exposed to the boiler at 750 °C. A thermogravimetric examination was conducted to evaluate the kinetics of corrosion. Corroded samples were examined with scanning electron microscopy and x-ray diffraction analysis after the end of the corrosion cycle. This research study concludes that CNT-reinforced coatings provide better corrosion resistance than conventional alumina coatings in the boiler environment.

### Keywords

Reinforced coatings; composites; ceramic matrix; carbon nanotubes; plasma spraying; T12 steel corrosion

### Introduction

Hot corrosion is an unwanted phenomenon in boilers of thermal power plants due to its high operating temperatures [1,2]. With the depletion of fossil fuels, the use of low-grade fuels is increasing in thermal power plants across the globe. The low-grade fuels contain impurities like Na, S, V and K elements, which react with oxygen at high temperatures of boilers, forming corrosive compounds such as Na<sub>2</sub>SO<sub>4</sub> or V<sub>2</sub>O<sub>5</sub>. These compounds are responsible for the initiation of corrosion in boiler components [3-6], which is accelerated at higher temperatures [2-3].

Thermal spray coatings have been used by various researchers to improve the corrosion resistance of boiler components. Among various available thermal spraying techniques, the plasma spraying technique has been used to deposit ceramic materials such as Al<sub>2</sub>O<sub>3</sub>, Cr<sub>2</sub>O<sub>3</sub>, TiO<sub>2</sub> and other similar materials on the boiler components [5,7]. Among various ceramic materials, alumina (Al<sub>2</sub>O<sub>3</sub>) is known for its high hardness and corrosion resistance even at higher temperatures like 1100 °C [8]. CNTs (carbon nanotubes) are nanofibers invented in 1991 with exceptional properties. These properties make CNTs a suitable reinforcement material for composites [9-10]. Thermal spray coatings are produced by melting powder particles, which solidify on the substrate. These layers of coatings

contain porosities and through holes, corrosive elements can attack the substrate and induce corrosion. Therefore, in the recent past, researchers have developed composite coatings by mixing CNTs in conventional powders and tried to decrease the porosity of developed coatings [11]. Therefore, there is a scope to develop new composite coatings with low porosities, which in turn can enhance the corrosion resistance of boiler components. In this experimental work CNTs reinforced alumina-titania coatings have been developed and corrosion resistance of these newly developed coatings has been evaluated in a boiler environment.

## Experimental

### *Test material and coating characterization*

Grade T12 steel used in boiler tubes is selected as substrate material. This material was procured from the Thermal Power Plant of North India. The specimens with 20×15×5 mm dimensions were prepared by cutting on an electrical discharge machine. The size of samples was cross-checked with a digital vernier caliper. The samples were polished with emery papers. The chemical composition of the steel checked at the CIDCO-IDFC, Chandigarh, is mentioned in Table 1.

**Table 1.** Chemical composition of T12 steel

ASME-code		Content, wt.%							
		C	Mn	Si	S	P	Cr	Mo	Fe
T-12	Nominal	0.05-0.15	0.3-0.6	0.5-1.00	0.025	0.025	0.8-1.25	0.44-0.65	Balance
	Actual	0.11	0.48	0.61	0.021	0.0214	0.941	0.27	Balance

A number of composite coatings were prepared by blending Al<sub>2</sub>O<sub>3</sub>, TiO<sub>2</sub> (size 40±10 μm) with 1.5 and 3 wt.% CNTs in a laboratory ball mill. The plasma spraying method was used to deposit the coatings on the substrates. The chemical composition of coating powders is given in Table 2.

**Table 2.** Chemical compositions and designations of coating powders

	Coating designation	Composite powder
Coating 1	0CAT	87.0 wt.% Al <sub>2</sub> O <sub>3</sub> + 13.0 wt.% TiO <sub>2</sub>
Coating 2	1.5CAT	85.5 wt.% Al <sub>2</sub> O <sub>3</sub> + 13.0 wt.% TiO <sub>2</sub> + 1.5 wt. % CNT
Coating 3	3CAT	84.0 wt.% Al <sub>2</sub> O <sub>3</sub> + 13.0 wt.% TiO <sub>2</sub> + 3.0 wt. % CNT

The SEM image and XRD of 84 wt.% Al<sub>2</sub>O<sub>3</sub> - 13 wt.% TiO<sub>2</sub> - 3 wt.% CNT are shown in Figures 1 and 2 to validate the authenticity of the powder used. The alumina and TiO<sub>2</sub> particles with the dispersed carbon nanotubes can be seen in the SEM image, as shown in Figure 1. The peaks of Al<sub>2</sub>O<sub>3</sub>, TiO<sub>2</sub>, and carbon can be clearly observed in the XRD analysis of the 3CAT powder shown in Figure 2.

Optimized standard process parameters were applied in the spraying process. These deposition parameters are listed in Table 3.

**Table 3.** Process parameters of plasma spraying

Plasma spraying parameters	Value
Arc current, A	550
Voltage, V	50
Pressure of Ar, kPa	400
Pressure of H <sub>2</sub> , kPa	60
Spray length, mm	90 to 110
RPM of hopper	1.5
Pressure of powder gas, kPa	300

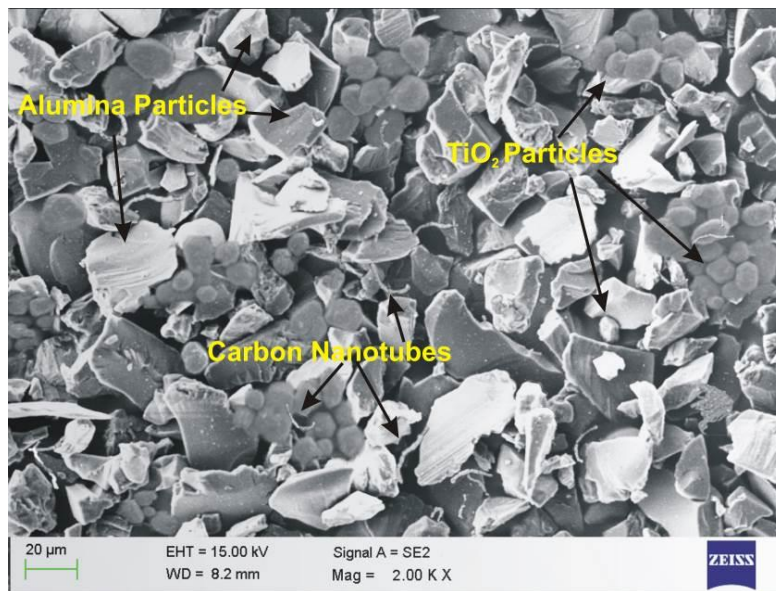


**Figure 1.** SEM image of 3CAT powder

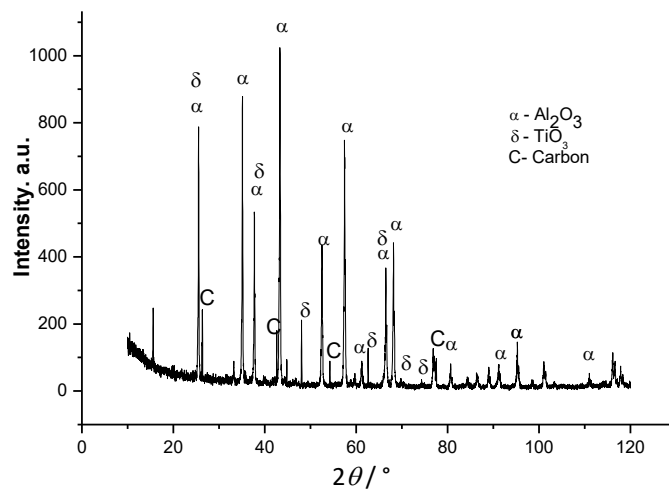


**Figure 2.** XRD peaks 3CAT powder

The thickness of the coating was found in the range of 250±5 μm, measured out from backscattered electron cross-sectional images, and shown in Figure 3 [12].

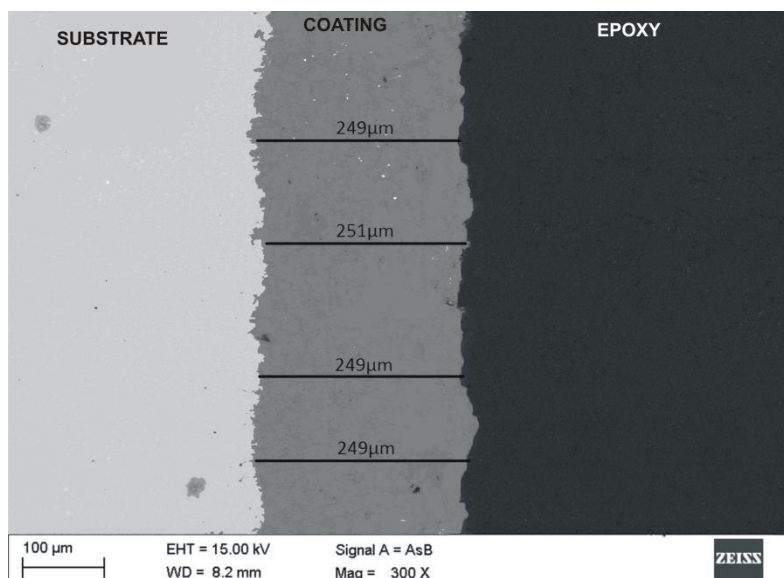


**Figure 3.** Cross-section image of as-sprayed coating

The porosity of Al<sub>2</sub>O<sub>3</sub>-TiO<sub>2</sub> coated specimen measured is more than 3 %, and it was reduced below 2.5 % on adding CNTs in Al<sub>2</sub>O<sub>3</sub>-TiO<sub>2</sub> powder. EDS analysis shown in Figure 4 shows uniformly dispersed CNTs in Al<sub>2</sub>O<sub>3</sub>-TiO<sub>2</sub> matrix in 3CAT coated steel.

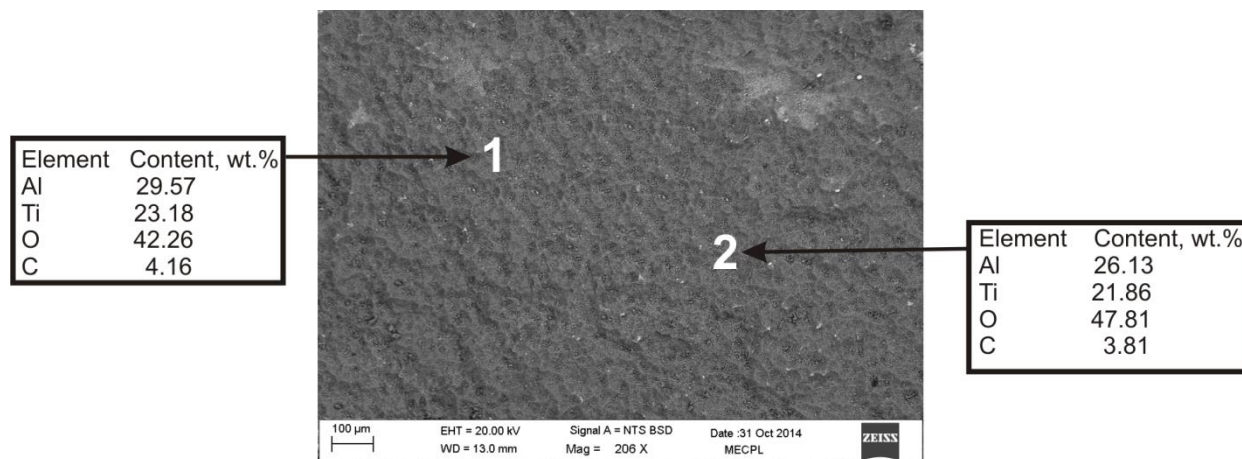


**Figure 4.** FE-SEM and EDS for 3CAT coated T12 boiler steel

### Hot corrosion analyses in the actual industrial environment

All substrates, bare as well as coated, were exposed in the actual boiler at the height of 31 m from its base, where the average temperature was around 750±10 °C. The samples were hung with a nichrome wire. The samples were weighed after every 100 hours of exposure for 10 cycles. This includes 1000 hours of heating inside the boiler at 750±10 °C. Degradation behaviour was evaluated utilizing cumulative weight gain and thickness loss. Corroded samples were analysed by XRD, SEM and EDS.

## Results

### Visual examination

All specimens were checked visually after each cycle of 100 hours of heating. After the completion of 10 cycles, the macrographs of all specimens were taken and shown in Figure 5 (a-d). The uncoated sample showed more degradation due to corrosion at high temperatures. Ash was stuck onto the sample after the completion of 1st cycle. The deposition of ash on the sample continued till the last cycle.

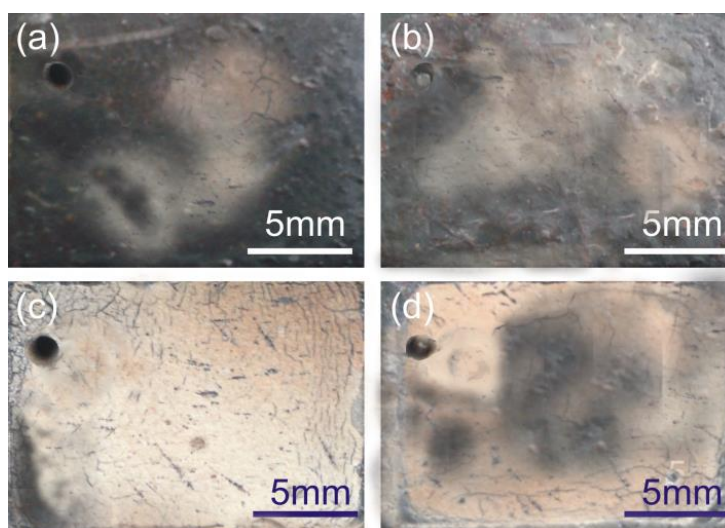


**Figure 5.** Macrographs of (a) bare steel, (b) 0CAT coating, (c) 1.5CAT coating, (d) 3CAT coating

This ash will be cleared off the sample by acetone washing. Following the completion of each cycle, the specimen weight was recorded. For the rest of the samples, a little spalling was observed in 0CAT coated steel in the 2<sup>nd</sup> cycle. For 1.5CAT and 3CAT coated samples, no spalling was observed after 1000 hours of cyclic study, and only ash deposition was observed.

#### Change in weight and loss of thickness information

Figure 6 shows the cumulative weight gain/unit area for all tested specimens following 1000 hours of cyclic testing. The overall weight gain, gain in weight caused by the formation of oxide scale and loss in weight is caused by scale spalling, for the bare T12 steel came out to be 147.51 and 102.21 mg/cm<sup>2</sup> for 0CAT coated T12 steel, and 51.24 and 24.58 mg/cm<sup>2</sup> for 1.5CAT and 3CAT coated T12 steel, respectively. The graph represents that CNT reinforcement has reduced the weight gain in coated steels.

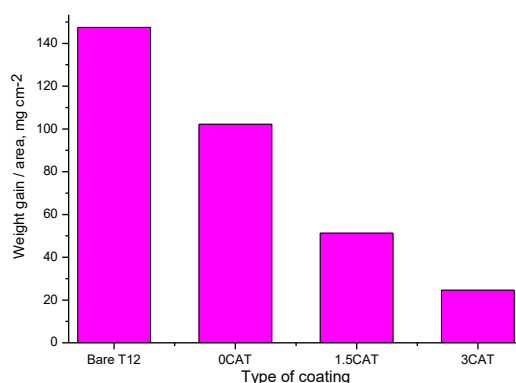


**Figure 6.** Cumulative weight gain per unit area for bare steel, 0CAT, 1.5CAT and 3CAT coatings

For a more accurate prediction of corrosion rate, the values are analyzed in mm year<sup>-1</sup>. The corrosion rate measured in terms of loss of thickness is shown in Table 4.

**Table 4.** Thickness loss

	Coating designation	Thickness loss, mm
Uncoated	Bare T12 Steel	0.8354
Coating 1	0CAT	0.3599
Coating 2	1.5CAT	0.0963
Coating 3	3CAT	0.0612

The corrosion rate for bare steel is 288.13 mpy. Further, the corrosion rates for 0CAT, 1.5CAT coated, and 3CAT coated steel were recorded as 124.11, 33.21 and 21.12 mm year<sup>-1</sup>, respectively, and are shown in Figure 7.

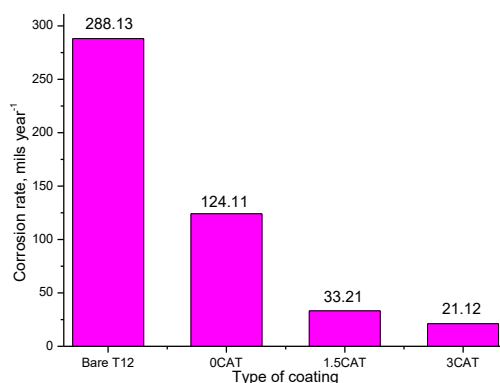


**Figure 7.** Corrosion rate for bare T12 steel, 0CAT, 1.5CAT and 3CAT coatings

### X-ray diffraction analysis

X-ray analysis for tested T12 samples after exposure is given in Figure 8. Bare steel has oxides of Fe, and ash SiO<sub>2</sub> (Figure 5a). 0CAT coated sample showed Al<sub>2</sub>O<sub>3</sub> and TiO<sub>2</sub> phase along with Na<sub>2</sub>O and SiO<sub>2</sub> (Figure 5b). For 1.5CAT, and 3CAT coated T12 steels, Al<sub>2</sub>O<sub>3</sub> and TiO<sub>2</sub> were the major phases and C, Na<sub>2</sub>O, and SiO<sub>2</sub> were the minor XRD phases (Figure 5 c-d).

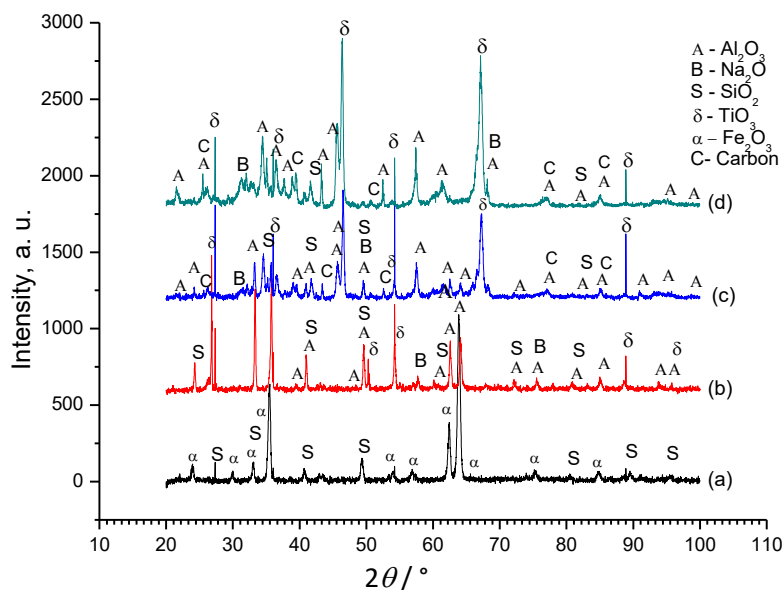


**Figure 8.** XRD pattern for the (a) bare, (b) 0CAT coated, (c) 1.5CAT coated, (d) 3CAT coated T12 steel after exposure

### FE-SEM and EDS analysis

This analysis for all samples after industrial exposure is shown in Figure 9. The surface micrograph of the uncoated sample indicated severe loss due to spalling and corrosion in Figure 9a. There are whitish and greyish regions. Erosion of the surface was also observed. EDS analysis at points 1 and 2 indicates that Si, Al, and O are present along with Fe. The presence of ash may be the reason for this. Hence the formation of Fe<sub>2</sub>O<sub>3</sub> and SiO<sub>2</sub> may be predicted. The micrograph of the 0CAT coated specimen (Figure 9b) shows that Al, Ti, Si, V and O elements are present at points 1 and 2. This predicts the formation of aluminum and titanium oxide layer and the ash. Higher amounts of Al and Ti were observed in the micrographs of 1.5CAT and 3CAT coated T12 steels (Figure 9c-d). Carbon (C) in a minor percentage is also visible due to the CNT presence in the coating matrix at both points.

### Discussion

A very thin scale that seems to be peeled off was observed for bare steel. The sample was eroded and spalled continuously throughout the experimentation. There was an ash deposition as the experimentation was done within the boiler. Therefore, spalling and erosion were a reason for the higher corrosion rate for bare steel.

The coal used in thermal plants has more than 30 % ash. This ash contains K<sub>2</sub>O and Na<sub>2</sub>O and reacts with boilers flue gases (SO<sub>2</sub>, SO<sub>3</sub> and O<sub>2</sub>). The authors [13-16] reported that this content of ash was rendered because of coal burning. Deposition of such low melting-point elements initiates hot corrosion on the boiler tube surface [17]. NaVO<sub>3</sub> is a deposit detected on boiler tubes with a low melting point and causes corrosion of boiler steel [18]. Further, K<sub>2</sub>SO<sub>4</sub>, and Na<sub>2</sub>SO<sub>4</sub> present in flue gases and ash react with Fe<sub>2</sub>O<sub>3</sub> and SO<sub>3</sub> and form trisulfide [19], and these sulphates cause corrosion in boiler steels [20]. The scale is spalled and restored on the surface of the boiler steel tube.

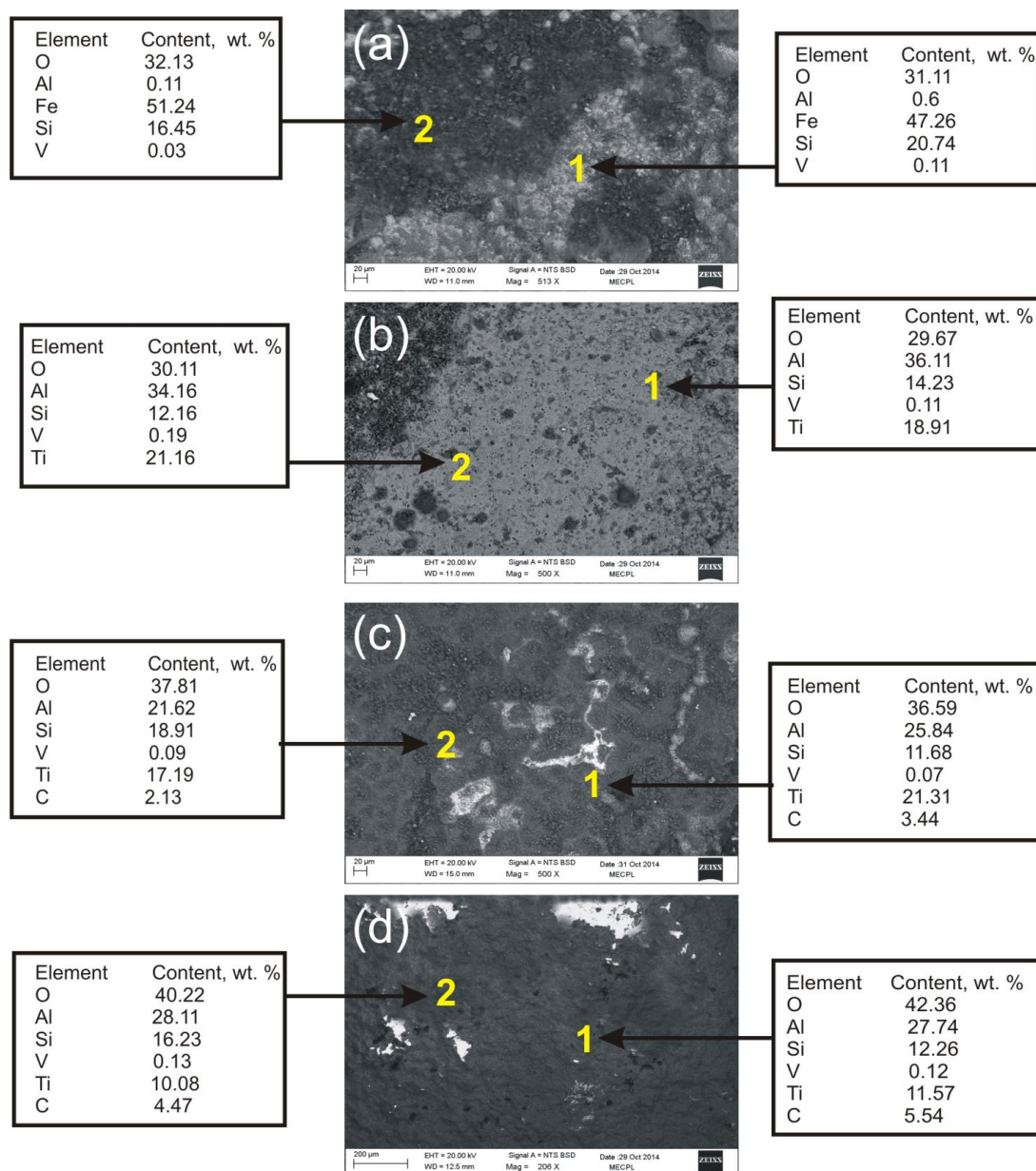


**Figure 9.** FE-SEM and EDS of (a) bare steel, (b) OCAT coating, (c) 1.5CAT coating, (d) 3CAT coating

XRD analysis depicts  $\text{Fe}_2\text{O}_3$  and  $\text{SiO}_2$  as the main phases in the case of bare T12 steel. The same has been reported by various researchers [21]. The corrosion rate of coated T12 steel is much lesser in comparison to bare steel.

The dense coating of alumina-titania present on T12 steel may be the reason for the increase in the degradation resistance. The same has been reported by authors [22-23].

CNT-reinforced alumina-titania coating was efficient in controlling degradation even after exposure to the boiler environment. 3CAT coated sample has shown maximum resistance to degradation. This may be due to the diminishing in porosity of the coating caused by CNT reinforcement into the main coating matrix. The coating with lesser porosity has more resistance to corrosion, as observed by the author [22]. XRD graphs showed the peaks for  $\text{TiO}_2$ ,  $\text{Al}_2\text{O}_3$  and  $\text{SiO}_2$  along with C in the scale, which has already been noticed by other authors [13]. The  $\text{SiO}_2$  phase may be because of ash particles present on the surface of a specimen. CNTs are responsible for reduced porosity and improved adhesion, which further decrease the corrosion rate [7,9]. A number of researchers [15,16] have reported similar findings in their studies on carbon nanotubes.

## Conclusions

- The bare T12 steel showed more corrosion after the cyclic testing.
- Coatings proved to help enhance the resistance to corrosion in the actual boiler environment.
- The better performance of 3CAT coated steel than 0CAT and 1.5CAT coated steels was due to CNT presence in the coating mixture.
- In the boiler environment, 3CAT coating on T12 steel was tested as the most effective and its thickness loss is only around 7.33 % of the uncoated T12 steel. This may be due to the formation of a less porous and compact structure due to CNT addition.

## References

- [1] S. Singh, K. Goyal, D. Bhandari, B. Krishan, *Journal of Bio-and Tribo-Corrosion* **7** (2021) 100. <https://doi.org/10.1007/s40735-021-00536-1>
- [2] P. Puri, K. Goyal, R. Goyal, B. Krishan, *Advanced Engineering Forum* **41** (2021) 43-54. <https://doi.org/10.4028/www.scientific.net/AEF.41.43>
- [3] V. P. Singh Sidhu, K. Goyal, R. Goyal, *Advanced Engineering Forum* **20** (2017) 1-9. <https://doi.org/10.4028/www.scientific.net/AEF.20.18>
- [4] V. Pal Singh, K. Goyal, R. Goyal, *Australian Journal of Mechanical Engineering* **17(2)** (2019) 127-132. <https://doi.org/10.1080/14484846.2017.1364834>
- [5] A. K. Keshri, V. Singh, J. Huang, S. Seal, W. Choi, A. Agarwal, *Surface and Coatings Technology* **204(11)** (2010) 1847-1855. <https://doi.org/10.1016/j.surfcoat.2009.11.032>
- [6] K. Goyal, *World Journal of Engineering* **16(1)** (2019) 64-70. <https://doi.org/10.1108/WJE-08-2018-0262>
- [7] K. Goyal, H. Singh, R. Bhatia, *Journal of the Australian Ceramic Society* **55** (2019) 315-322. <https://doi.org/10.1007/s41779-018-0237-9>
- [8] Q. Ding, X.-F. Tang, Z.-G. Yang, *Engineering Failure Analysis* **73** (2017) 129-138. <https://doi.org/10.1016/j.engfailanal.2016.12.011>
- [9] K. Goyal, H. Singh, R. Bhatia, *International Journal of Minerals, Metallurgy and Materials* **26** (2019) 337-344. <https://doi.org/10.1007/s12613-019-1742-8>
- [10] H.S. Sidhu, B. S. Sidhu, S. Prakash, *Journal of Materials Processing Technology* **171(1)** (2006) 77-82. <https://doi.org/10.1016/j.jmatprotec.2005.06.058>
- [11] R. Kumar, D. Bhandari, K. Goyal, *Materials Performance and Characterization* **11(1)** (2022). <http://dx.doi.org/10.1520/MPC20210080>
- [12] B. Bhushan, B. K. Gupta, *Handbook of Tribology: Materials, coatings, and surface treatments*, New York: McGraw-Hill, 1991. ISBN: 0070052492 9780070052499
- [13] J. Stokes, L. Looney, *Surface and Coatings Technology* (**177-178**) (2004) 18-23. <https://doi.org/10.1016/j.surfcoat.2003.06.003>
- [14] R. Kumar, D. Bhandari, K. Goyal, *Journal of Electrochemical Science and Engineering* **12(4)** (2022) 651-666. <http://dx.doi.org/10.5599/jese.1190>
- [15] K. Goyal, R. Goyal, *Surface Engineering* **36(11)** (2020) 1200-1209. <https://doi.org/10.1080/02670844.2019.1662645>
- [16] K. Goyal, H. Singh, R. Bhatia, *Journal of the Australian Ceramic Society* **55** (2019) 315-322. <https://doi.org/10.1007/s41779-018-0237-9>
- [17] A. Portinha, V. Teixeira, J. Carneiro, J. Martins, M. Costa, R. Vassen, D. Stoeber, *Surface and Coatings Technology* **195(2-3)** (2005) 245-251. <https://doi.org/10.1016/j.surfcoat.2004.07.094>
- [18] T. Sidhu, S. Prakash, R. Agrawal, *Journal of Materials Engineering and Performance* **15** (2006) 122-129. <https://doi.org/10.1361/105994906X83402>

- [19] K. Szymański, A. Hernas, G. Moskal, H. Myalska, *Surface and Coatings Technology* **268** (2015) 153-164. <https://doi.org/10.1016/j.surfcoat.2014.10.046>
- [20] K. Balani, T. Zhang, A. Karakoti, W. Li, S. Seal, A. Agarwal, *Acta Materialia* **56(3)** (2008) 571-579. <https://doi.org/10.1016/j.actamat.2007.10.038>
- [21] S. Kumar, M. Kumar, A. Handa, *Materials at High Temperatures* **37(6)** (2020) 370-384. <https://doi.org/10.1080/09603409.2020.1810922>
- [22] E. H. Jordan, M. Gell, Y. H. Sohn, D. Goberman, L. Shaw, S. Jiang, M. Wang, T. D. Xiao, Y. Wang, P. Strutt, *Materials Science and Engineering: A* **301(1)** (2001) 80-89. [https://doi.org/10.1016/S0921-5093\(00\)01382-4](https://doi.org/10.1016/S0921-5093(00)01382-4)
- [23] A. Portinha, V. Teixeira, J. Carneiro, J. Martins, M. Costa, R. Vassen, D. Stoeber, *Surface and Coatings Technology* **195(2-3)** (2005) 245-251. <https://doi.org/10.1016/j.surfcoat.2004.07.094>

